Fracture behavior of bainitic and pearlitic rail steel webs

H. AGLAN*, M. HASSAN, Z. LIU, M. BHUYAN
Mechanical Engineering Department, Tuskegee University, Tuskegee, AL 36088
E-mail: aglanh@tuskegee.edu

M. FATEH
Federal Railroad Administration, 1120 Vermont Ave. N. W., Washington, DC 20590, USA

The failure of railway rail occurs mainly due to processes such as: detail fracture, shelling, and transverse fissures [1]. Plastic deformation of the railhead due to the heavy rolling loads transmitted through the wheel/rail contact surface is the main reason for the formation of detail fracture [2]. Such a failure process is visible, and catastrophic rail failure can be prevented by regular examination of the top surface of the railhead. The fracture behavior of railheads has been studied for a long time and some significant results have been obtained [3–8]. The study of the failure of rail webs is less reported. In webs, defect accumulation may occur under cyclic service loadings. Once the crack size reaches the sub-critical dimension, piping propagation along the vertical direction of the web can be accelerated, while the cyclic vertical tension loads can cause horizontal fissures of the web. Considering the complexity of the failure modes related to the cyclic loadings of rail tracks, it is necessary to study the fracture behavior of rail webs under a simplified loading profile first.

Recently an improved bainitic steel for heavy load application has been studied [9–12]. It has some significant benefits over the existing pearlitic rail steels. Bainitic steels derive their strength from ultra-fine structures with a lot of dislocations which are harmless but confer high strength [13]. In contrast, pearlitic steels obtain their strength from the fine grains of pearlite. However, there is a limit to the production of very fine grains in the manufacturing and post-heat treatment processes.

In the present work, the fracture behavior of specimens cut from bainitic and pearlitic steel rail webs was studied. An empirical model of mode I stress intensity factor was used to evaluate the plane strain fracture toughness of the two materials. Rail web specimens from the two materials, with simulated cracks emanating from a trough thickness circular defect, were prepared by electric discharge machining to simulate horizontal fissure of rail webs. Static tensile tests were performed under displacement control to study the overloading behavior and obtain the residual strength for the plane strain fracture toughness calculation based on this geometry.

The rails used in the present work were new (have not been in service) and were supplied by the Transportation Technology Center, Inc. (TTCI), Pueblo, Colorado. The composition range of the pearlitic steel, controlled in accordance with the American Railway Engineering and Maintenance-of-Way Association (AREMA) Manual is given in Table I [14]. The composition of the bainitic rail steel as determined by the Colorado Metallurgical Services [15] is also given in Table I. The rail web was cut vertically into 6.3 mm thick plates by electric discharge machining (EDM). The dimension of the tensile test specimens of bainitic rail web was 150 mm length by 17.3 mm width. The dimension of the tensile specimens of pearlitic rail web was 110 mm length by 16.3 mm width. In the middle of the specimens, a 3 mm diameter hole was drilled, following which, two 1.6 mm notches for bainitic rail web and two 1.0 mm notches for pearlitic rail web, emanating from the hole, were introduced by EDM. A photo showing how the specimens were machined from the rail web is shown in Fig. 1. Static tensile experiments under displacement control were performed using Materials Testing System 810 equipped with a 100 kN load cell. The specimens were gripped between two hydraulic wedge grips type 647.10A-01. The gauge length for both materials was 4 times the specimen width. The fracture surfaces were examined using scanning electron microscopy (SEM).

Considering the case of cracks emanating from a hole in a rectangular plate under tension as depicted in Fig. 2, the general expression of stress intensity factor is as follows [16, 17]:

$$K = F \cdot \sigma \sqrt{\pi a} \tag{1}$$

where σ is the remote stress, a is half of the crack length and F is a geometrical correction factor. In order to calculate, F, a series of geometrical constants are defined, which include:

$$\alpha = \frac{a}{W}, \quad \bar{\alpha} = \frac{\pi}{2}\alpha, \quad \delta = \frac{a}{R},$$
$$\gamma = \frac{R}{W} \quad \text{and} \quad \beta = \frac{\alpha - \gamma}{1 - \gamma}.$$

According to Fuhring [18], the geometrical correction factor in Equation 1 can be expressed as:

$$F = \varphi \cdot \psi \tag{2}$$

*Author to whom all correspondence should be addressed.

0022–2461

TABLE I Composition of the railheads

Element	C	Mn	P	S	Si	Ni	Cr	Cu	Mo	V
Pearlitic rail	0.72–0.78	0.60–1.25	0.035	0.037	0.1–0.6	0.25	0.25–0.5		0.1	0.03–0.05
Bainitic rail	0.23	1.93	0.012	0.008	1.96	0.14	1.84	0.13	0.43	0.007

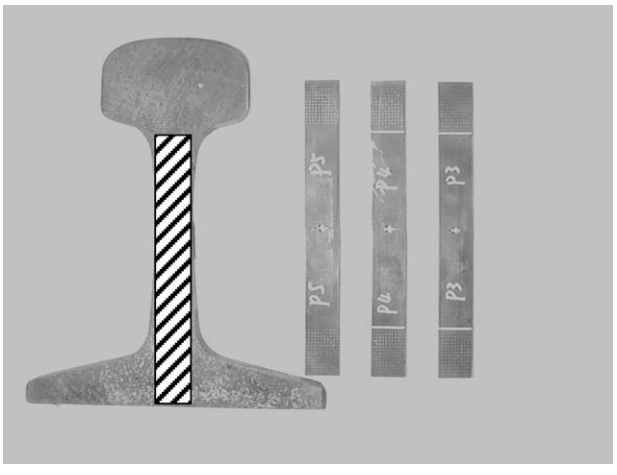

Figure 1 Rail web test specimens.

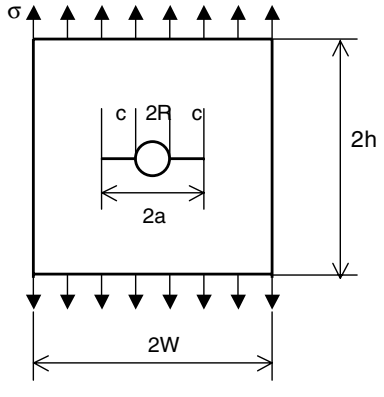

Figure 2 Schematic illustration of a finite plate with two symmetrical cracks emanatings from a through thickness circular hole.

φ and ψ can be expressed as:

$$\varphi = \frac{\pi\left[\sqrt{\frac{1}{\bar{\alpha}}(\tan\bar{\alpha} + g\cdot\sin 2\bar{\alpha})}\cdot\left(1+\frac{\varepsilon^2(2-\varepsilon^2)}{1-\varepsilon}\right)\right] - \sqrt{1+2g}}{\pi - 1} \tag{3a}$$

$$\psi = \xi\cdot\left(3\beta^{\frac{2}{3}P} - 2\sqrt{\xi}\beta^{P}\right). \tag{3b}$$

The parameters in Equations 3a and 3b can be defined as:

$$g = 0.13\left(\frac{2}{\pi}\cdot\arctan\delta\right)^2 \tag{4}$$

$$\varepsilon = \alpha\cdot\frac{2}{\pi}\cdot\arctan(0.6\sqrt[3]{\delta}) \tag{5}$$

$$P = \frac{\log\left(\frac{1}{\xi^{\frac{3}{2}}}\right)}{\log\beta^*} \tag{6}$$

In Equation 6 $\beta^* = \frac{\gamma\cdot\delta}{\gamma(2\delta-1)+1}$, and $\xi = 1 + \frac{2}{\pi}\arctan(1.5\cdot\sqrt{\delta})$.

In this work, the specimens from bainitic rail web have $R = 1.5$ mm, $c = 1.6$ mm, $a = R + c = 3.1$ mm, $W = 8.65$ mm. Therefore, the csalculated values of $\alpha = \frac{a}{W} = 0.358$, $\bar{\alpha} = 0.563$, $\delta = 2.067$, $\gamma = 0.173$, $\beta = 0.224$, $\beta^* = 0.232$, and $\xi = 1.724$. Thus, applying these values in the expression of g, ε and P gives,

$$g = 0.13\left(\frac{2}{\pi}\cdot\arctan\delta\right)^2 = 0.066,$$

$$\varepsilon = \alpha\cdot\frac{2}{\pi}\cdot\arctan\left(0.6\sqrt[3]{\delta}\right) = 0.149, \quad \text{and}$$

$$P = \frac{\log\left(\frac{1}{\xi^{\frac{3}{2}}}\right)}{\log\beta^*} = 0.559.$$

Substituting the values of g, ε and P into Equations 3a and 3b yields: $\varphi = 1.212$ and $\psi = 1$. Therefore, the value of the geometrical correction factor for the bainitic steel specimen is $F = 1.212$.

The pearlitic rail web specimens have $R = 1.5$ mm, $c = 1.0$ mm, $a = R + c = 2.5$ mm, $W = 8.1$ mm. Therefore, the calculated values of $\alpha = \frac{a}{W} = 0.309$, $\bar{\alpha} = 0.485$, $\delta = 1.667$, $\gamma = 0.185$, $\beta = 0.152$, $\beta^* = 0.215$, $\xi = 1.697$, $g = 0.06$, $\varepsilon = 0.122$, $P = 0.516$, $\varphi = 1.159$ and $\psi = 0.992$. Therefore, the value of the geometrical correction factor for the pearlitic steel specimens is F 1.15.

The residual tensile strength was calculated based on the original cross-sectional area without the central hole and emanating initial notches. The average residual tensile strength for the bainitic rail web reached about 790 MPa, while that for the pearlitic rail web was 450 MPa. In this study, the geometric correction factor F of the bainitic specimen is 1.212 as calculated above, from which the average calculated plane strain fracture toughness, K_I is 95 MPa$\sqrt{m}$. The value of F for the pearlitic web specimens is 1.15, yielding an average plane strain fracture toughness, K_I of 41 MPa$\sqrt{m}$. The value of K_I for pearlitic rail steel agrees very well with those reported by Dhua *et al.* [19]. These workers investigated six commercial heats of pearlitic rail steel and found that their fracture toughness range was from 42 to 50 MPa$\sqrt{m}$. Thus, the fracture toughness of the bainitic rail steel is more than twice that of the pearlitic rail steel. It should be mentioned that these values are for plane strain fracture toughness and are considerably lower than those for plane stress fracture toughness, as reported earlier for both materials [20, 21].

The higher strength and toughness of the bainitic steel can be related to the distribution of carbide particles; the strength increases by increasing the number of carbide particles. As the bainite transformation

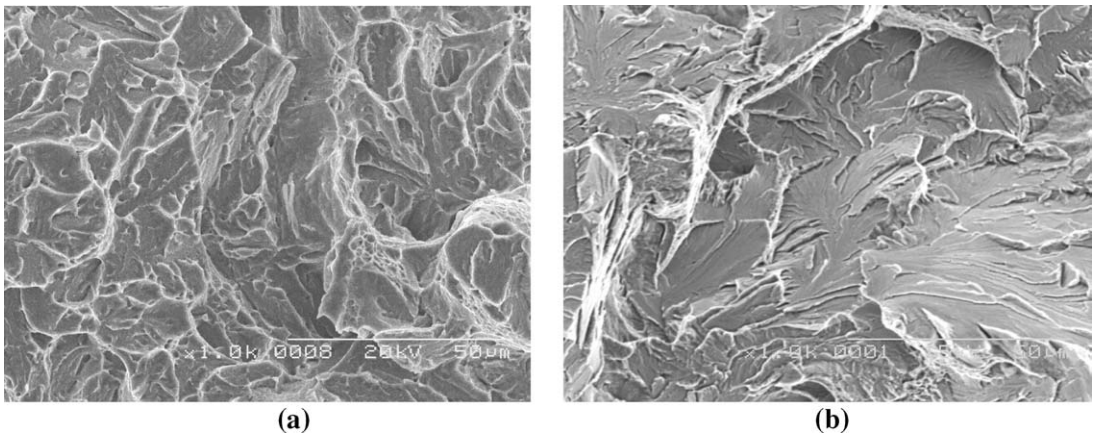

Figure 3 SEM micrographs showing the fracture morphology of both rail webs: (a) Bainitic rail web and (b) Pearlitic rail web.

temperature is decreased, the carbides will be dispersed; the size of carbide particles will be small and the number of carbides in the plane section will be large, therefore the strength will increase greatly. However, the dispersed carbides, as effective barriers to dislocation glide, retard the motion of dislocation, so the ductile strain is decreased. It should be mentioned here that the bainitic rail web attains its superior mechanical properties despite its lower carbon content through the bainite phase, which is obtained with the help of certain alloying elements and a specific cooling procedure, compared to the relatively high carbon content in the pearlitic rail web.

The fracture surface morphology, immediately ahead of the crack tip, of typical specimens from the bainitic and the pearlitic rail webs was examined and is shown in Fig. 3a and b, respectively. The notch tip is on the left side of these micrographs, i.e., the crack traveled from left to right. At 1000×, the micrographs display different fracture features. The bainitic fracture displays ductile tearing features and plastic deformation. This is manifested by tearing ridges and pulled-up strips. Dimples are evident on the bainitic fracture surface, Fig. 3a, but hardly seen on the pearlitic rail web surface, Fig. 3b. On the other hand, the pearlitic steel, Fig. 3b, displays cleavage facets and river patterns covering most of the fracture surface. The frequent transgranular cleavage can be the reason for the relative increase of brittleness of the pearlitic rail steel. These apparent differences in the fracture damage species explain the fracture toughness superiority of the bainitic rail steel.

Comparative studies on the plane strain fracture toughness of bainitic and pearlitic rail webs revealed that the bainitic K_{I} value is more than two fold that of the pearlitic rail web. The average K_{I} values for the bainitic and pearlitic rail webs, were 95 MPa$\sqrt{m}$ and 41 MPa$\sqrt{m}$, respectively. This fracture toughness superiority of the bainitic rail steel is manifested in the more ductile failure mechanisms seen on the fracture surface of the bainitic rail steel. More dimples and tearing is seen on the bainitic surface as compared to cleavage facets seen on the pearlitic fracture surface.

Acknowledgment

This work was sponsored by the Federal Railroad Administration (FRA), Department of Transportation. The authors thank Mr. Gunars, Spons of FRA, for facilitating the contact with TTCI to provide the material and training for the Tuskegee University team.

References

1. D. H. STONE, *Canadian Metall. Quart.* **21**(1) (1982) 17.
2. G. J. FOWLER and A. S. TETELMAN, in "Rail Steels-Development, Processing, and Use, ASTM STP644," edited by D. H. Stone and G. G. Knupp (American Society for Testing and Materials, 1978) p. 363.
3. U. P. SINGH, R. SINGH and S. BANERJEE, *Scand. J. Metall.* **24**(5/6) (1995) 237.
4. I. VITEZ, *Metalurgija* **35**(1) (1996) 49.
5. D. H. TOBIAS and D. A. FOUTCH, *Struct. Engng. Rev.* **7**(3) (1995) 231.
6. D. Y. JEONG, *Theor. Appl. Fract. Mechan.* **22**(1) (1995) 43.
7. Y. CHENG, D. CHEN and F. NOGATA, *Fatigue Fract. Engng. Mater. Struct.* **17**(1) (1994) 113.
8. Y. MURAKAMI and S. HAMADA, *ibid.* **20**(6) (1997) 863.
9. D. DAVIS, M. SCHOLL and D. GUILLEN, *Techn. Dig.* TD97-049 (1997).
10. H. YOKOYAMA, S. MITAOA, S. YAMAMOTOA and M. FUJIKAKEB, *Wear* **253** (2002) 60.
11. P. CLAYTON and X. SU, *ibid.* **200** (1996) 63.
12. P. CLAYTON, *ibid.* **191** (1996) 170.
13. K. J. SAWLEY, *Techn. Dig.* TD97-001 (1997).
14. American Railway Engineering Assoc., *AREA Manual Railway Engng.* (1997) 4.
15. J. KRISTAN, TTCI, Pueblo, CO, private communication.
16. G. R. IRWIN, *J. Appl. Mech.* **24** (1957) 361.
17. K. HELLAN, "Introduction to Fracture Mechanics" (McGraw-Hill Book Company, New York, 1984) p. 244.
18. H. FUHRING, *Int. J. Fract.* **9** (1973) 328.
19. S. K. DHUA, A. RAY, S. K. SEN, M. S. PRASAD, K. B. MISHRA and S. JHA, *J. Mater. Engng. Perform.* **9**(6) 2000 700.
20. A. M. KHOURSHID, Y. X. GAN and H. A. AGLAN, *ibid.* **10** (2001) 331.
21. H. AGLAN, Z. LIU and M. HASSAN, *ibid.* in press.

Received 22 December 2003
and accepted 11 February 2004